

# The simplified hybrid-combined methods for Laplace's equation with singularities \*

Z.C. LI \*\* and T.D. BUI

*Department of Computer Science, Concordia University, 1455 de Maisonneuve Blvd. West, Montréal, Québec, Canada H3G 1M8*

Received 10 July 1988

Revised 4 April 1989

**Abstract:** In Li and Liang (1983), the simplified hybrid-combined method is presented for combining the Ritz–Galerkin method and the finite-element method. In this paper we will apply this method to solve singularity problems of Laplace's equation. Error bounds and stability analyses will be provided while taking into account the integration approximation along the coupling boundary. A significant coupling relation between the Ritz–Galerkin and the finite-element method has been found for the Laplace equation with singularities. An optimal rate of convergence has also been achieved. Numerical experiments have been carried out for solving the benchmark problem: Motz's problem to verify the theoretical results.

**Keywords:** Singularity problems, combined methods, hybrid methods, finite-element methods, the Ritz–Galerkin methods, elliptic boundary value problems.

## 1. Introduction

There have appeared many singularity problems involving elliptic equations, such as angular singularity problems, interface problems and unbounded domain problems, from scientific research and engineering applications. Since the traditional finite-element method (FEM) and finite-difference method both cause a reduced convergence rate of the numerical solutions [22], the study on innovated numerical methods for singularity problems is significant. Numerous approaches have been reported over the past twenty years. Here we cite some important methods:

1. The conformal transformation method of Whiteman and Papamichael in 1972 [24]. This method uses a conformal transformation to remove the singularity of solutions.
2. The nonuniform FEM. Near the singular point, very small elements are used to decrease the errors resulting from singularity. A theoretical analysis is given in [7].

\* This work was supported in part by the Natural Sciences and Engineering Research Council of Canada under Grant No. A9265 and B94, the Fonds pour la Formation de Chercheurs et l'Aide à la Recherche of Québec under Grant No. EQ-2904 and by the Ministère de l'Enseignement Supérieur et de la Science (Action structurante).

\*\* Centre de Recherche Informatique de Montréal, Inc., 1550 de Maisonneuve Blvd. West, Bureau 901, Montréal, Québec, Canada H3G 1N2.

3. The infinite-grid refinement method of Thatcher [23] and Han [9] for simple equations, such as the Laplace equation. The small elements in Method 2 could approach those with arbitrarily small boundary length.
4. The coupling method of the boundary-element method (BEM) and FEM. The singular points are dealt with by BEM; the rest of the solution domain is still treated by FEM [10,28].
5. The nonlocal boundary condition method of Goldstein [8] for unbounded domain problems. Other promising approaches are:
6. Adding the singular functions into FEM. See the singular function methods of Fix et al. [6], Strang and Fix [22], and the dual singular function method of Blum and Dobrowolski [3].
7. Subtracting singular expansions from FEM solutions by Wigley [26]. This is a reverse process of 6.

The above methods all are based on the solutions of FEM. Nevertheless, there also exist the approaches using piecewise particular solutions (or expansions) only. For instance:

8. The T-complete boundary method of Zielinski and Zienkiewicz [27].
9. The global-element method of Delves and Hall [5].
10. The boundary methods of Li [14] and Li et al. [19].
11. The *hp*-version of FEM of Babuška and Guo [2].

The approaches in 10 and 11 provide an exponential rate of convergence. In this paper, we shall follow the ideas presented in 12.

12. The nonconforming combinations of Li [12–14]. Particular solutions and FEM are used separately in the neighbourhood region of the singular points and the rest of the solution domain. A nonconforming, constraint condition is imposed on the common boundary  $\Gamma_0$  of two subdomains.

Since the coupling techniques are very important, we study the techniques of additional integrals along  $\Gamma_0$  to couple two different methods, instead of the constraint condition in [12–14]. To achieve this, we use the following approach:

13. The hybrid-combined methods of Li and Bui [16], and Li and Liang [18]. In particular, theoretical analysis of the variation crimes is presented in this paper.

Other kinds of additional integrals are given by:

14. Penalty and hybrid methods of Li and Bui [15–17].

For solving homogeneous elliptic boundary-value problems, the simplified hybrid-combined method is provided [18] for combining the Ritz–Galerkin method and FEM. Such a coupling strategy is equivalent to that of [28] for combining the boundary-element method and FEM. Let the solution domain  $S$  be divided into  $S_1$  and  $S_2$  by an artificial boundary  $\Gamma_0$ , i.e.,  $S = S_1 \cup S_2$  and  $\Gamma_0 = \partial S_1 \cap \partial S_2$ . The FEM is used in  $S_1$  where the true solution is smooth enough; the Ritz–Galerkin method is used in  $S_2$  where the true solution may have singular property. Since suitable singular functions can approximate the true solution very well near the singular point, the combination of the Ritz–Galerkin and FEM will produce numerical solutions with optimal convergence rates as long as a suitable coupling strategy along  $\Gamma_0$  can be found. Such a combination is given in [18] where the simplified hybrid integral along  $\Gamma_0$  is capable of coupling different numerical methods.

However, from the point of view of practical application, further studies into the simplified hybrid-combined method have to be done. For instance, we have to approximate the simplified hybrid integral on  $\Gamma_0$ , to choose an empirical coupling relation between the Ritz–Galerkin method and FEM and in particular, to perform some numerical experiments that can verify the theoretical analyses. All these are the purposes of this paper.

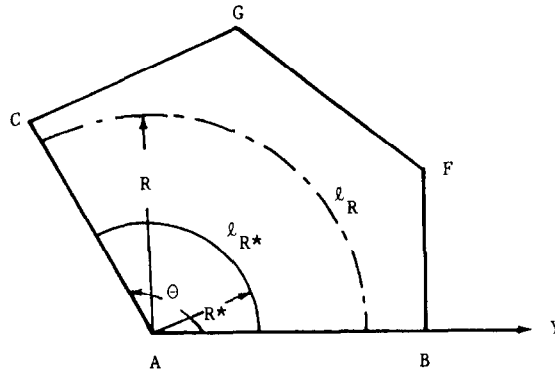


Fig. 1. The angular singularity problem of Laplace's equation.

Let us consider a typical Laplace equation with Dirichlet–Neumann boundary conditions [13,14] (see Fig. 1):

$$\Delta u = \frac{\partial^2 u}{\partial x^2} + \frac{\partial^2 u}{\partial y^2} = 0, \quad (x, y) \in S, \quad (1.1)$$

$$u = 0, \quad (x, y) \in \overline{AC}, \quad (1.2)$$

$$\frac{\partial u}{\partial n} = 0, \quad (x, y) \in \overline{AB}, \quad (1.3)$$

$$\frac{\partial u}{\partial n} = g, \quad (x, y) \in \overline{BF} \cup \overline{FG} \cup \overline{GC}, \quad (1.4)$$

where  $n$  is the outward normal of  $\Gamma$ , and  $g$  is sufficiently smooth on the boundary  $\overline{BF} \cup \overline{FG} \cup \overline{GC}$ . Equations (1.1)–(1.4) can be written in the following weak form:

$$A(u, v) = g(v), \quad \forall v \in H_0^1(S), \quad u \in H_0^1(S), \quad (1.5)$$

where the bilinear form is

$$A(u, v) = \int \int_S (u_x v_x + u_y v_y) \, dS, \quad (1.6)$$

$$g(v) = \int_{\overline{BF} \cup \overline{FG} \cup \overline{GC}} g v \, dl, \quad (1.7)$$

$$H_0^1(S) = \{v \mid v, v_x, v_y \in L^2(S) \text{ and } v|_{\overline{AC}} = 0\}. \quad (1.8)$$

We note that there exists a singular point at the origin  $(0, 0)$ , resulting from the intersection of the Dirichlet–Neumann boundary conditions when the angle  $\Theta = \angle CAB \neq \pi/2k$ ,  $k$  are integers. Because of the singularity of solutions, the traditional or finite-difference method causes a reduced convergence rate of the numerical solutions. An idea arises naturally that a combination of the Ritz–Galerkin and FEM or the Ritz–Galerkin and finite-difference method will be a good approach for singularity problems.

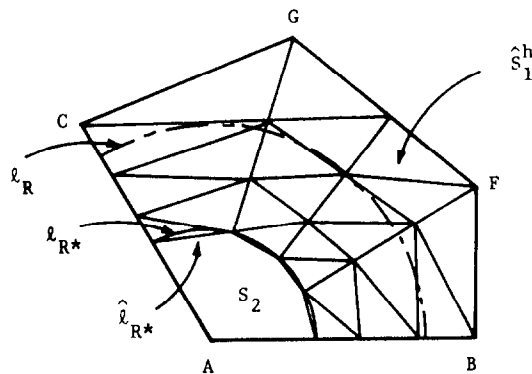


Fig. 2. The division of the solution domain for the simplified hybrid-combined method.

Expansions of solutions near the origin  $(0, 0)$ :

$$u(r, \theta) = \sum_{l=0}^{\infty} D_l \left( \frac{r}{R} \right)^{\sigma(l+\frac{1}{2})} \cos \sigma(l+\frac{1}{2})\theta, \quad r \leq R, \quad (1.9)$$

have been found in [11,22,25], where  $D_l$  are expansion coefficients,  $(r, \theta)$  are polar coordinates with the origin  $(0, 0)$ , i.e., the singular point, and  $\sigma = \pi/\Theta$ . Then

$$u(R, \theta) = \sum_{l=0}^{\infty} D_l \cos \sigma(l+\frac{1}{2})\theta, \quad (1.10)$$

with the expansion coefficients

$$D_l = \frac{2}{\Theta} \int_0^{\Theta} u(R, \theta) \cos \sigma(l+\frac{1}{2})\theta \, d\theta. \quad (1.11)$$

Based on the expansion (1.9), it is convenient to choose the coupling boundary  $\Gamma_0$  to be a circular arc  $l_{R^*}$  ( $r = R^*$ ,  $0 \leq \theta \leq \Theta$ ) with the condition

$$R^* < R. \quad (1.12)$$

In this case, the subdomain  $S_2$  is a sector ( $r < R^*$ ,  $0 < \theta < \Theta$ ); and  $S_1$  is the rest of  $S$ . (See Fig. 2.)

Admissible functions in the combination are chosen as

$$v = \begin{cases} v^+ = \sum_{l=0}^L \hat{D}_l \left( \frac{r}{R} \right)^{\sigma(l+\frac{1}{2})} \cos \sigma(l+\frac{1}{2})\theta & \text{in } S_2, \\ v^- = v_1 & \text{in } \hat{S}_1^h, \end{cases} \quad (1.13)$$

where  $\hat{D}_l$  are unknown coefficients to be solved,  $\hat{S}_1^h$  is the triangulation domain of  $S_1$ , (then  $\hat{S}_1^h \approx S_1$ ), and  $v_1$  are piecewise linear interpolation functions on  $\hat{S}_1^h$ . We note that there exists a small, overlapped region

$$\text{Area}(S_2 \cap \hat{S}_1^h) \neq 0$$

in (1.13). This is a kind of variation crimes, but it does not cause a reduced rate of convergence.

Such a definition as (1.13) will lead to the simplicity of both algorithms and error analysis below.

Let  $V_h^0$  denote the space of the admissible functions  $v$ , then

$$V_h^0 \notin H^1(S) \quad (1.14)$$

owing to the noncontinuity of  $v$  on  $\Gamma_0$ , i.e.,  $l_{R^*}$ . The simplified hybrid-combined method is designed to seek an approximate solution  $u_h \in V_h^0$ , such that

$$A_h(u_h, v) = g(v), \quad \forall v \in V_h^0, \quad (1.15)$$

where the bilinear form is

$$A_h(u, v) = \int \int_{\hat{S}_1^h} \nabla u \nabla v \, dS + \int \int_{S_2} \nabla u \nabla v \, dS + \int_{\Gamma_0} \left[ \frac{\partial u^+}{\partial n} v^- - \frac{\partial v^+}{\partial n} u^- \right] dl, \quad (1.16)$$

where  $n$  is the outward normal to  $\partial S_2$ , and

$$v^+ = v|_{\Gamma_0^+}, \quad v^- = v|_{\Gamma_0^-}. \quad (1.17)$$

It is remarkable that the simplified hybrid integral on  $\Gamma_0$

$$I_S = \int_{\Gamma_0} \left[ \frac{\partial u^+}{\partial n} v^- - \frac{\partial v^+}{\partial n} u^- \right] dl \quad (1.18)$$

plays a role of coupling the Ritz–Galerkin method and FEM.

In practical calculations, the integral  $I_S$  cannot be computed exactly, and has to be approximated by some integration rules, e.g., by the simplest, trapezoidal rule

$$\int_{\xi}^{\xi+\Delta\xi} f(\xi) \, d\xi \approx \frac{1}{2} \Delta\xi [f(\xi) + f(\xi + \Delta\xi)]. \quad (1.19)$$

Then we have

$$\begin{aligned} I_S &\approx \hat{I}_S = \int_{\Gamma_0} \left[ \frac{\partial u^+}{\partial n} v^- - \frac{\partial v^+}{\partial n} u^- \right] dl \\ &= \sum_{i=0}^N \left[ \frac{\partial u^+(R^*, \theta_j)}{\partial r} v^-(R^*, \theta_j) - \frac{\partial v^+(R^*, \theta_j)}{\partial r} u^-(R^*, \theta_j) \right] \frac{1}{2} R^* (\Delta\theta_j + \Delta\theta_{j-1}), \end{aligned} \quad (1.20)$$

where  $\Delta\theta_j = \theta_{j+1} - \theta_j$  and  $\Delta\theta_N = \Delta\theta_{-1} = 0$ .

Let  $\hat{u}_h$  denote the numerical solution concerning the integration approximation (1.20), and then

$$\hat{A}_h(\hat{u}_h, v) = g(v), \quad \forall v \in V_h^0, \quad (1.21)$$

where

$$\hat{A}_h(u, v) = \int \int_{\hat{S}_1^h} \nabla u \nabla v \, dS + \int \int_{S_2} \nabla u \nabla v \, dS + \int_{\Gamma_0} \left( \frac{\partial u^+}{\partial n} v^- - \frac{\partial v^+}{\partial n} u^- \right) dl. \quad (1.22)$$

Compared with the method given in [18], there exist two kinds of variation crimes. This is the terminology of Strang and Fix [22]; (1) the integration approximation (1.20), and (2) the small overlap of  $\hat{S}_1^h$  and  $S_2$ ; (otherwise, complicated, isoparametric elements must be employed [4]).

Below, we shall estimate error bounds of the solution  $\hat{u}_h \in V_h^0$  by (1.21) with the variation crimes, (1) and (2).

## 2. Error bounds and coupling strategy

Since  $V_h^0 \notin H^1(S)$ , we define a norm over  $V_h^0$ :

$$\|v\|_h = \left( \|v\|_{1,S_1^h}^2 + \|v\|_{1,S_2}^2 \right)^{\frac{1}{2}}. \quad (2.1)$$

We shall assess the errors of solutions, in the norm  $\|\cdot\|_h$ .

We need two lemmas.

**Lemma 1.** *Let the family of all triangular elements in  $\hat{S}_1^h$  be regular (see [4]) with a maximal length  $h$ , and let the true solution  $u$  satisfy*

$$\frac{\partial u}{\partial r} \in H^2(\Gamma_0). \quad (2.2)$$

*Also assume that the integration points  $(R^*, \theta_j)$  in (1.20) are the element nodes on the common boundary  $\Gamma_0$ , (i.e.,  $l_{R^*}$ ) and the circular arcs  $\Gamma_0^j$  ( $r = R^*$ ,  $\theta_j \leq \theta \leq \theta_{j+1}$ ) fall into only one triangular element  $\Delta_i$  in  $\hat{S}_1^h$ , i.e.,  $\Gamma_0^j \in \Delta_i$ . Then for the trapezoidal integration approximation (1.20), there exist bounds*

$$\left| \int_{\Gamma_0} \frac{\partial u}{\partial n} w^- \, dl - \hat{\int}_{\Gamma_0} \frac{\partial u}{\partial n} w^- \, dl \right| \leq C \frac{H^2}{\sqrt{h}} \left\| \frac{\partial u}{\partial r} \right\|_{2,\Gamma_0} \|w\|_{1,\hat{S}_1^h}, \quad \forall w \in V_h^0, \quad (2.3)$$

where  $H$  is the maximal mesh spacing of integration nodes, e.g.,  $H = R^* \max_j \Delta\theta_j$ , and  $C$  is a bounded constant independent of  $h$ ,  $H$ ,  $L$ ,  $u$ . (The values of  $C$  may be different in different contexts.)

**Proof.** For the trapezoidal rule, we have

$$\begin{aligned} \left| \int_{\Gamma_0} \frac{\partial u}{\partial n} w^- \, dl - \hat{\int}_{\Gamma_0} \frac{\partial u}{\partial n} w^- \, dl \right| &\leq CH^2 \sum_j \left| \frac{\partial u}{\partial n} w^- \right|_{2,\Gamma_0^j} \\ &\leq CH^2 \left\| \frac{\partial u}{\partial n} \right\|_{2,\Gamma_0} \left( \|w^-\|_{0,\Gamma_0}^2 + \|w^-\|_{1,\Gamma_0}^2 + \sum_j \|w^-\|_{2,\Gamma_0^j}^2 \right)^{\frac{1}{2}}, \end{aligned} \quad (2.4)$$

where  $\Gamma_0^j$  denotes a small circular arc ( $r = R^*$ ,  $\theta_j \leq \theta \leq \theta_{j+1}$ ). We note that the norms  $\|w^-\|_{2,\Gamma_0^j}$  exist since the admissible, piecewise linear interpolation functions  $w^-$  on  $\Gamma_0^j$  are sufficiently smooth by means of the assumption  $\Gamma_0^j \in \Delta_i$ .

Bounds can be found in [12] for the piecewise linear interpolation function  $w^-$

$$\|w^-\|_{2,\Gamma_0^j} \leq C \|w^-\|_{1,\Gamma_0^j}, \quad (2.5)$$

$$\|w^-\|_{1,\Gamma_0} \leq C \frac{1}{\sqrt{h}} \|w^-\|_{1,\hat{S}_1^h}. \quad (2.6)$$

Then, we have from the Sobolev imbedding theorem [21] and the Poincaré–Friedrichs inequality [4]

$$\|w^-\|_{0,\Gamma_0}^2 + \|w^-\|_{1,\Gamma_0}^2 + \sum_j \|w^-\|_{2,\Gamma_0^j}^2 \leq C \frac{1}{h} \|w\|_{1,S_h^h}^2. \quad (2.7)$$

The desired result (2.3) follows from (2.2), (2.4) and (2.7).  $\square$

**Lemma 2.** Suppose that  $H$  and  $L$  satisfy

$$\left[\sigma\left(L + \frac{1}{2}\right)\right]^{\frac{1}{2}} H \leq C. \quad (2.8)$$

Then there exist bounds

$$|\hat{A}_h(u, v)| \leq C \|u\|_h \|v\|_h. \quad (2.9)$$

**Proof.** On the basis of (1.22), we obtain

$$\begin{aligned} |\hat{A}_h(u, v)| &\leq \left| \int_{S_1^h} \nabla u \nabla v \, dS + \int_{S_2^h} \nabla u \nabla v \, dS + \int_{\Gamma_0} \frac{\partial u^+}{\partial n} v^- \, dl - \int_{\Gamma_0} \frac{\partial v^+}{\partial n} u^- \, dl \right| \\ &\quad + \left| \int_{\Gamma_0} \frac{\partial u^+}{\partial n} v^- \, dl - \hat{\int}_{\Gamma_0} \frac{\partial u^+}{\partial n} v^- \, dl \right| + \left| \int_{\Gamma_0} \frac{\partial v^+}{\partial n} u^- \, dl - \hat{\int}_{\Gamma_0} \frac{\partial v^+}{\partial n} u^- \, dl \right|. \end{aligned} \quad (2.10)$$

Since  $u^+$  and  $v^+$  in (1.13) are all particular solutions of the homogeneous Laplace equation, we can see from the trace theorem [20] and the Sobolev imbedding theorem [21] (also see Babuška and Aziz [1,p.32])

$$\left| \int_{\Gamma_0} \frac{\partial u^+}{\partial n} v^- \, dl \right| \leq C \left\| \frac{\partial u^+}{\partial n} \right\|_{-\frac{1}{2},\Gamma_0} \|v^-\|_{\frac{1}{2},\Gamma_0} \leq C' \|u\|_{1,S_2^h} \|v\|_{1,S_h^h}, \quad (2.11a)$$

$$\left| \int_{\Gamma_0} \frac{\partial v^+}{\partial n} u^- \, dl \right| \leq C \left\| \frac{\partial v^+}{\partial n} \right\|_{-\frac{1}{2},\Gamma_0} \|u^-\|_{\frac{1}{2},\Gamma_0} \leq C' \|v\|_{1,S_2^h} \|u\|_{1,S_h^h}, \quad (2.11b)$$

where  $C'$  is also a bounded constant independent of  $L$ ,  $h$ ,  $H$ ,  $u$  and  $v$ .

On the other hand, the approximate integration  $\hat{\int}_{\Gamma_0}$  can be regarded as  $\int_{\Gamma_0}$  but with the substitution of the integrands, such as  $(\partial u^+/\partial n)v^-$  or  $(\partial v^+/\partial n)u^-$  by their piecewise linear interpolation functions along  $\Gamma_0$ . We then have from Strang and Fix [22],

$$\left| \int_{\Gamma_0} \frac{\partial u^+}{\partial n} v^- \, dl - \hat{\int}_{\Gamma_0} \frac{\partial u^+}{\partial n} v^- \, dl \right| \leq CH \left| \frac{\partial u^+}{\partial n} v^- \right|_{1,\Gamma_0}. \quad (2.12)$$

Also using [1,21] yields

$$\left| \frac{\partial u^+}{\partial n} v^- \right|_{1,\Gamma_0} \leq C \left\| \frac{\partial u^+}{\partial r} \right\|_{\frac{1}{2},\Gamma_0} \|v^-\|_{\frac{1}{2},\Gamma_0} \leq C' \left\| \frac{\partial u^+}{\partial r} \right\|_{\frac{1}{2},\Gamma_0} \|v\|_{1,S_h^h}. \quad (2.13)$$

By noting the expansions (1.13) of  $v^+$  and the orthogonality of trigometric functions, we can obtain

$$\begin{aligned} & \left\| \frac{\partial u^+}{\partial r} \right\|_{2, \Gamma_0}^2 \\ &= \int_0^\Theta \left[ \left( \frac{1}{R^{*2}} \frac{\partial^3 u^+}{\partial \theta^2 \partial r} \right)^2 + \left( \frac{1}{R^*} \frac{\partial^2 u^+}{\partial \theta \partial r} \right)^2 + \left( \frac{\partial u^+}{\partial r} \right)^2 \right] R^* d\theta \\ &= \frac{\Theta}{2} \sum_{l=0}^L \hat{D}_l^2 \left( \frac{R^*}{R} \right)^{\sigma(2l+1)} \left\{ \frac{1}{R^{*5}} [\sigma(l + \frac{1}{2})]^6 + \frac{1}{R^{*3}} [\sigma(l + \frac{1}{2})]^4 + \frac{1}{R^*} [\sigma(l + \frac{1}{2})]^2 \right\}, \end{aligned} \quad (2.14a)$$

and (see [13])

$$\iint_{S_2} \left( \frac{1}{r} \frac{\partial u^+}{\partial \theta} \right)^2 dS = \frac{\Theta}{4} \sum_{l=0}^L \hat{D}_l^2 \sigma(l + \frac{1}{2}) \left( \frac{R^*}{R} \right)^{\sigma(2l+1)}. \quad (2.14b)$$

It follows that

$$\left\| \frac{\partial u^+}{\partial r} \right\|_{2, \Gamma_0} \leq C [\sigma(L + \frac{1}{2})]^{\frac{1}{2}} \left\{ \iint_{S_2} \left( \frac{1}{r} \frac{\partial u^+}{\partial \theta} \right)^2 dS \right\}^{\frac{1}{2}} \leq C [\sigma(L + \frac{1}{2})]^{\frac{1}{2}} \|u^+\|_{1, S_2}. \quad (2.15)$$

Finally from (2.12), (2.13) and (2.15) we obtain

$$\left| \int_{\Gamma_0} \frac{\partial u^+}{\partial n} v^- dl - \hat{\int}_{\Gamma_0} \frac{\partial u^+}{\partial n} v^- dl \right| \leq C [\sigma(L + \frac{1}{2})]^5 H \|u\|_{1, S_2} \|v\|_{1, \hat{S}_1^h}. \quad (2.16a)$$

Similarly, we obtain

$$\left| \int_{\Gamma_0} \frac{\partial v^+}{\partial n} u^- dl - \hat{\int}_{\Gamma_0} \frac{\partial v^+}{\partial n} u^- dl \right| \leq C [\sigma(L + \frac{1}{2})]^5 H \|v\|_{1, S_2} \|u\|_{1, \hat{S}_1^h}. \quad (2.16b)$$

The desired result (2.9) follows from (2.8), (2.10), (2.11) and (2.16).  $\square$

**Theorem 3.** *Let all conditions in Lemmas 1 and 2 hold, and  $\text{meas}(\overline{AC} \cap \partial \hat{S}_1^h) \neq 0$ . Then there exist error bounds*

$$\begin{aligned} \|u - \hat{u}_h\|_h \leq C & \left\{ \inf_{v \in V_h^0} \|u - v\|_h + \sup_{w \in V_h^0} \frac{\left| \hat{\int}_{\Gamma_0} \frac{\partial u}{\partial r} w^- dl - \int_{\Gamma_0} \frac{\partial u}{\partial r} w^- dl \right|}{\|w\|_h} \right. \\ & \left. + \sup_{w \in V_h^0} \frac{\left| \int_{\Gamma_0} \frac{\partial u}{\partial r} w^- dl - \int_{\hat{\Gamma}_0} \frac{\partial u}{\partial n} w^- dl \right|}{\|w\|_h} \right\}, \end{aligned} \quad (2.17)$$

where  $\hat{\Gamma}_0$  is the exterior boundary of  $\hat{S}_1^h$ , i.e.,  $\hat{\Gamma}_0 \approx \Gamma_0$ , and  $n$  is the inward normal to  $\partial \hat{S}_1^h$ .



**Proof.** In the simplified hybrid-combined method (1.21), we note that the functions  $v$  in  $\hat{S}_1^h$  and  $v$  in  $S_2$  are arbitrary and independent to each other. We then have

$$\int \int_{\hat{S}_1^h} \nabla u \nabla v \, dS + \int_{\Gamma_0} \frac{\partial u^+}{\partial r} v^- \, dl = g(v), \quad (2.18)$$

$$\int \int_{S_2} \nabla u \nabla v \, dS - \int_{\Gamma_0} \frac{\partial v^+}{\partial r} u^- \, dl = 0. \quad (2.19)$$

Since the functions  $u^+$  and  $v^+$  both satisfy the Laplace equation in  $S_2$ , (2.19) reduces to

$$\int_{\Gamma_0} \frac{\partial u^+}{\partial r} v^+ \, dl = \int_{\Gamma_0} \frac{\partial v^+}{\partial r} u^+ \, dl = \hat{\int}_{\Gamma_0} \frac{\partial v^+}{\partial r} u^- \, dl. \quad (2.20)$$

Now let  $u$  be a true solution of (1.1)–(1.4) or (1.5), we then obtain

$$\begin{aligned} \hat{A}_h(u, v) &= \int_{\partial \hat{S}_1^h} \frac{\partial u}{\partial n} v^- \, dl + \int_{\partial S_2} \frac{\partial u}{\partial n} v^+ \, dl + \hat{\int}_{\Gamma_0} \left( \frac{\partial u}{\partial r} v^- - \frac{\partial v^+}{\partial r} u \right) \, dl \\ &= - \int_{\hat{\Gamma}_0} \frac{\partial u}{\partial n} v^- \, dl + \int_{\Gamma_0} \frac{\partial u}{\partial r} v^+ \, dl + \hat{\int}_{\Gamma_0} \left( \frac{\partial u}{\partial r} v^- - \frac{\partial v^+}{\partial r} u \right) \, dl + g(v) \\ &= - \int_{\hat{\Gamma}_0} \frac{\partial u}{\partial n} v^- \, dl + \hat{\int}_{\Gamma_0} \frac{\partial u}{\partial r} v^- \, dl + g(v), \end{aligned} \quad (2.21)$$

where  $\hat{\Gamma}_0$  is the interior boundary of  $\partial \hat{S}_1^h$  and  $\hat{\Gamma}_0 \approx \Gamma_0$ . In the last step in (2.21), we have applied the equality (2.20).

Next, with the help of the assumption of

$$\text{meas}(\overline{AC} \cap \partial \hat{S}_1^h) \neq 0 \quad \text{and} \quad \text{meas}(\overline{AC} \cap \partial S_2) \neq 0,$$

that holds true naturally, we can see from the Poincaré–Friedrichs inequality [4]

$$C_0 \|v\|_{1, \hat{S}_1^h}^2 \leq \|v\|_{1, \hat{S}_1^h}^2, \quad C_0 \|v\|_{1, S_2}^2 \leq \|v\|_{1, S_2}^2, \quad (2.22)$$

where  $C_0$  is a positive constant independent of  $L$ ,  $h$ ,  $H$  and  $v$ . Therefore, the following uniformity  $V_h^0$ -elliptic inequality holds:

$$C_0 \|v\|_h^2 \leq \|v\|_{1, \hat{S}_1^h}^2 + \|v\|_{1, S_2}^2 = \hat{A}_h(v, v). \quad (2.23)$$

Below, we let  $v \in V_h^0$ , then combining (2.23), (2.21) and (1.21) gives

$$\begin{aligned} C_0 \|v - \hat{u}_h\|_h^2 &\leq \hat{A}_h(v - \hat{u}_h, v - \hat{u}_h) \\ &= \hat{A}_h(v - \hat{u}_h, v - u) + \int_{\hat{\Gamma}_0} \frac{\partial u}{\partial n} w^- \, dl - \hat{\int}_{\Gamma_0} \frac{\partial u}{\partial r} w^- \, dl, \end{aligned} \quad (2.24)$$

with  $w = u - \hat{u}_h \in V_h^0$ .

Moreover, we can see from Lemma 2

$$\hat{A}_h(v - \hat{u}_h, v - u) \leq C \|v - \hat{u}_h\|_h \|v - u\|_h. \quad (2.25)$$

Also it follows from (2.24) and (2.25) that

$$\begin{aligned} (2.25) \quad & \left| \int_{\hat{\Gamma}_0} \frac{\partial u}{\partial n} w^- \, dl - \int_{\hat{\Gamma}_0} \frac{\partial u}{\partial r} w^- \, dl \right| \\ & \leq \left| \int_{\Gamma_0} \frac{\partial u}{\partial r} w^- \, dl - \int_{\hat{\Gamma}_0} \frac{\partial u}{\partial n} w^- \, dl \right| + \left| \int_{\Gamma_0} \frac{\partial u}{\partial r} w^- \, dl - \int_{\hat{\Gamma}_0} \frac{\partial u}{\partial r} w^- \, dl \right|. \end{aligned} \quad (2.26)$$

Finally, we obtain from (2.24)–(2.26)

$$\begin{aligned} (2.27) \quad & C_0 \|v - \hat{u}_h\| \leq C \|v - u\|_h \\ & + \frac{1}{\|w\|_h} \left\{ \left| \int_{\Gamma_0} \frac{\partial u}{\partial r} w^- \, dl - \int_{\hat{\Gamma}_0} \frac{\partial u}{\partial n} w^- \, dl \right| + \left| \int_{\Gamma_0} \frac{\partial u}{\partial r} w^- \, dl - \int_{\hat{\Gamma}_0} \frac{\partial u}{\partial r} w^- \, dl \right| \right\}, \end{aligned} \quad (2.27)$$

and the desired bounds (2.17) result from (2.27) and the trigonometric inequality

$$\|u - \hat{u}_h\|_h \leq \|u - v\|_h + \|v - \hat{u}_h\|_h. \quad \square \quad (2.28)$$

In Theorem 3, the second term on the right side of (2.17) is an error resulting from the approximation integration; and the third term is an error resulting from the noncoincidence of  $\Gamma_0$  and  $\hat{\Gamma}_0$ , i.e., of  $S_1$  and  $\hat{S}_1^h$ .

**Theorem 4.** Let all conditions in Theorem 3 hold. Also suppose that  $u \in H^2(\hat{S}_1^h)$ , and (1.12) are satisfied. Then, there exist bounds

$$\|u - \hat{u}_h\|_h \leq C \left\{ h + \frac{H^2}{\sqrt{h}} + \left( \frac{R^*}{R} \right)^{\sigma(L+\frac{1}{2})} \right\}. \quad (2.29)$$

**Proof.** Define a trial function  $\bar{w} \in V_h^0$  such that

$$(2.30) \quad \bar{w} = \begin{cases} \bar{w}^+ = \sum_{l=0}^L D_l \left( \frac{r}{R} \right)^{\sigma(l+\frac{1}{2})} \cos \sigma(l+\frac{1}{2})\theta & \text{in } S_2, \\ u_1 & \text{in } S_1, \end{cases} \quad (2.30)$$

where  $D_l$  are the expansion coefficients defined by (1.11), and  $u_1$  are piecewise linear interpolation functions of  $u$  on  $\hat{S}_1^h$ . Then

$$u = \bar{w}^+ + \mathbb{R}_L \quad \text{in } S_2, \quad (2.31)$$

with the remainder term

$$(2.32) \quad \mathbb{R}_L = \sum_{l=L+1}^{\infty} D_l \left( \frac{r}{R} \right)^{\sigma(l+\frac{1}{2})} \cos \sigma(l+\frac{1}{2})\theta. \quad (2.32)$$

As a result, we have

$$\begin{aligned} (2.33) \quad & \inf_{v \in V_h^0} \|u - v\|_h \leq \|u - \bar{w}\|_h \leq \|u - u_1\|_{1, S_1^h} + \|u - \bar{w}^+\|_{1, S_2} \\ & \leq Ch \|u\|_{2, S_1^h} + \|\mathbb{R}_L\|_{1, S_2} \leq C \|u\|_{2, S_1^h} + C \left( \frac{R^*}{R} \right)^{\sigma(L+\frac{1}{2})}. \end{aligned} \quad (2.33)$$

Besides, we can see from Lemma 1 and [12]

$$\left| \int_{\Gamma_0} \frac{\partial u}{\partial r} w^- \, dl - \int_{\Gamma_0} \frac{\partial u}{\partial r} w^- \, dl \right| \leq C \frac{H^2}{\sqrt{h}} \left\| \frac{\partial u}{\partial r} \right\|_{2, \Gamma_0} \|w\|_{1, S_1^+} \quad (2.34)$$

and

$$\left| \int_{\Gamma_0} \frac{\partial u}{\partial r} w^- \, dl - \int_{\Gamma_0} \frac{\partial u}{\partial n} w^- \, dl \right| \leq Ch^2 \|w\|_{1, S_1^+} \quad (2.35)$$

We therefore obtain from Theorem 3

$$\|u - \hat{u}_h\|_h \leq C \left\{ h \|u\|_{2, S_1^+} + h^{\frac{1}{2}} + \frac{H^2}{\sqrt{h}} \left\| \frac{\partial u}{\partial r} \right\|_{2, \Gamma_0} + \|R_L\|_{1, S_2} \right\} \quad (2.36)$$

Since  $D_l = O(1/(\sigma(l + \frac{1}{2})))$  (see [13]), using (1.12) and the orthogonality of the trigonometric functions  $\cos \sigma(l + \frac{1}{2})\theta$  yields

$$\|R_L\|_{1, S_2}^2 = \frac{1}{2} \Theta \sum_{l=L+1}^{\infty} D_l^2 \left( \frac{R^*}{R} \right)^{\sigma(2l+1)} \left[ \sigma \left( l + \frac{1}{2} \right) + \frac{R^{*2}}{2 + \sigma(2l+1)} \right] \leq C \left( \frac{R^*}{R} \right)^{\sigma(2L+3)} \quad (2.37)$$

The bounds (2.29) are then obtained by combining (2.36) and (2.37).  $\square$

In (2.29), the bounds  $O(H^2/\sqrt{h})$  are the errors that come from the integration approximation (1.20).

Theorem 4 will lead to  $h$ -estimates for the errors of  $\|u - \hat{u}_h\|_h$ . The exploration of  $h^2$ -estimates for the errors in the  $L^2$ -norm needs to be done because the duality techniques of Aubin–Nitsche type [4,22] cannot be applied directly for the admissible functions  $v^+$  that satisfy exactly the homogeneous equation:  $\Delta u = 0$  in  $S_2$ .

In order to obtain the optimal convergence rate from (2.29), we shall consider the following

$$\|u - \hat{u}_h\|_h = O(h), \quad (2.38)$$

the following two conditions should be satisfied:

$$\frac{H^2}{\sqrt{h}} \leq Ch, \quad (2.39)$$

$$\left( \frac{R^*}{R} \right)^{\sigma(L+1)} = C_1 h. \quad (2.40a)$$

Equation (2.40a) leads to

$$L+1 = \frac{\ln C_1 h}{\sigma \ln \left( \frac{R^*}{R} \right)} - \frac{1}{2}. \quad (2.40b)$$

where  $C_1$  is a bounded constant independent of  $L$ ,  $h$ ,  $H$  and  $u$ .

As usual, let

$$H = O(h). \quad (2.41)$$

As the assumption in Lemma 1, we always choose the element nodes  $(R^*, \theta_j)$  on  $\Gamma_0$  as the integration points in (1.20). Then (2.39) holds from (2.41), and the condition (2.8) in Lemma 2 is automatically satisfied from (2.40) and (2.41).

We have the following corollary.

**Corollary 5.** *Let all conditions in Theorem 4 hold. Then there exists the optimal convergence rate (2.38) provided that both (2.40) and (2.41) are satisfied.*

Moreover, we obtain from [13] the next corollary.

**Corollary 6.** *Let (2.41) and all conditions in Theorem 4 hold. There then exists the optimal convergence rate (2.38) provided that the following coupling strategy between  $L_h + 1$  and  $h$  is applied:*

$$L_h + 1 = (L_{h_0} + 1) + \frac{\left| \ln \left( \frac{h}{h_0} \right) \right|}{\left| \sigma \ln \left( \frac{R^*}{R} \right) \right|}, \quad (2.42)$$

or

$$L_{\frac{1}{2}h} + 1 = (L_h + 1) + 1, \quad (2.43)$$

for a special case of  $\Theta = \pi$ , i.e.,  $\sigma = \pi/\Theta = 1$ , and  $R^*/R = \frac{1}{2}$ , where  $L_h + 1$  is the total number of expansion functions in  $S_2$ , corresponding to a fixed, maximal boundary length  $h$  of quasi-uniform elements in  $\hat{S}_1^h$ .

### 3. Solution methods and stability analyses

From (1.21), we can obtain linear algebraic equation systems

$$Bv + Ed = b_1, \quad -E^T v + Dd = 0, \quad (3.1)$$

where  $v$  is the unknown vector with the components  $v_{ij}$ , and the approximate solutions  $v$  on the elements nodes  $(i, j)$  in  $\hat{S}_1^h$ ,  $d$  is the unknown vector with coefficients  $\hat{D}_l$ ,  $b_1$  is a known vector, and  $B$ ,  $D$ ,  $E$ ,  $E^T$  are matrices.  $E^T$  is the transposed matrix of  $E$ .

The matrices  $B$  and  $D$  are obtained from the integrals  $\iint_{\hat{S}_1^h} \nabla u \nabla v \, dS$  and  $\iint_{S_2} \nabla u \nabla v \, dS$  in (1.22), respectively. Let

$$\text{meas}(\overline{AC} \cap \partial \hat{S}_1^h) \neq 0, \quad (3.2)$$

the coefficient matrix  $B$  of the linear finite-element method is positive definite, symmetric and sparse. However, the matrix  $D$  is not only positive definite, symmetric, but also diagonal! In fact, since the circular arc  $l_{R^*}$  is chosen as the coupling boundary  $\Gamma_0$ , we let

$$u^+ = \sum_{l=0}^L \hat{D}_l \left( \frac{r}{R} \right)^{\sigma(l+\frac{1}{2})} \cos \sigma(l+\frac{1}{2})\theta \quad \text{and} \quad v^+ = \left( \frac{r}{R} \right)^{\sigma(k+\frac{1}{2})} \cos \sigma(k+\frac{1}{2})\theta. \quad (3.3)$$

Using the orthogonality of trigonometric functions yields

$$\int \int_{S_2} \nabla u \nabla v \, dS = \int_{\partial S_2} \frac{\partial u}{\partial n} v \, dl = \int_{\Gamma_0} \frac{\partial u^+}{\partial r} v^- \, dl = \frac{1}{2} \Theta \sum_{l=0}^L \hat{D}_l \sigma(l + \frac{1}{2}) \left( \frac{R^*}{R} \right)^{\sigma(2l+1)}. \quad (3.4)$$

Then, the matrix  $D$  has components

$$D = (d_{i,j})_{(L+1) \times (L+1)}, \quad (3.5)$$

where

$$d_{i,j} = 0 \quad \text{when } i \neq j, \quad d_{i,i} = \frac{1}{2} \Theta \sigma(i - \frac{1}{2}) \left( \frac{R^*}{R} \right)^{\sigma(2i-1)}. \quad (3.6)$$

It is due to the diagonal matrix  $D$  that the solution methods for (3.1) become much simpler. For instance, we solve (3.1) by

$$\mathbf{d} = D^{-1} E^T \mathbf{v}, \quad F \mathbf{v} = \mathbf{b}_1, \quad (3.7)$$

where the coefficient matrix

$$F = B + E D^{-1} E^T \quad (3.8)$$

is positive definite, symmetric and sparse because the matrix  $E D^{-1} E^T$  is symmetric and sparse. It is due to the positive definite matrices  $F$  and  $D$  that the solutions  $\mathbf{v}$  and  $\mathbf{d}$  in the discrete problem (3.7) (i.e., (3.1)) exist uniquely.

The stability can be measured by the condition numbers of the coefficient matrices  $F$  (and  $D$ ), defined by

$$\text{con. num.}(F) = \frac{\lambda \max(F)}{\lambda \min(F)}, \quad (3.9)$$

where  $\lambda \max(F)$  and  $\lambda \min(F)$  are the maximal and minimal eigenvalues of the matrix  $F$ , respectively. We have the next theorem.

**Theorem 7.** *Let the admissible functions (1.13) be given. Suppose (2.41) and (3.2) to be satisfied, and  $(R^*, \theta_j)$  in (1.20) to be the element nodes on  $l_{R^*}$ . Then, there exist bounds*

$$\text{con. num.}(D) \leq \frac{\left( \frac{R}{R^*} \right)^{2\sigma L}}{2L+1}, \quad \text{con. num.}(F) \leq C \left( \frac{1+hL^2}{h^2} \right), \quad (3.10)$$

where  $h$  is the maximal boundary length of regular elements in  $\hat{S}_1^h$ .

**Proof.** The left estimate in (3.10) can be obtained directly from (3.6):

$$\text{con. num.}(D) = \frac{d_{1,1}}{d_{L+1,L+1}} = \frac{\left( \frac{R}{R^*} \right)^{2\sigma L}}{2L+1}. \quad (3.11)$$

From (3.8) we have

$$\text{con. num.}(F) \leq \frac{\lambda \max(B) + \lambda \max(E D^{-1} E^T)}{\lambda \min(B)}. \quad (3.12)$$

Since  $B$  is the coefficient matrix coming from the linear finite element method, the assumption (3.2) gives [22]

$$(3.13) \quad \lambda \min(B) \geq C_0 h^2, \quad \lambda \max(B) \leq C, \quad (3.13)$$

where  $C_0$  and  $C$  are positive constants independent of  $h$ . The right estimate in (3.10) follows from the bounds

$$(3.14) \quad \lambda \max(ED^{-1}E^T) \leq ChL^2. \quad (3.14)$$

Let us prove (3.14) below.

In fact, the matrix  $E^T$  results from the integral  $\int_{l_{R^*}} (\partial v^+ / \partial r) u^- dl$ , whose values can be found by substituting  $v^+$  with (3.3):

$$(3.15) \quad \begin{aligned} \int_{l_{R^*}} \frac{\partial v^+}{\partial r} u^- dl &= \sum_{j=0}^N \frac{\partial v^+}{\partial r} (R^*, \theta_j) u_{0,j} \frac{1}{2} (R^* (\Delta \theta_j + \Delta \theta_{j+1})) \\ &= \sum_{j=0}^N \left( \frac{R^*}{R} \right)^{\sigma(l+\frac{1}{2})} \sigma(l+\frac{1}{2}) \cos(\sigma(l+\frac{1}{2})\theta_j) \frac{1}{2} (\Delta \theta_j + \Delta \theta_{j+1}) u_{0,j}, \end{aligned} \quad (3.15)$$

where the coefficient matrix  $E^T$  is symmetric and sparse because the matrix  $A$  is symmetric and sparse where  $u_{0,j} = u_{0,j} = u(R^*, \theta_j)$ ; subscripts  $(0, j)$  denote the nodes on  $l_{R^*}$ . Therefore, the matrix  $E^T$  is

$$(3.16) \quad E^T = (0, (E^*)^T), \quad (3.16)$$

where  $(E^*)^T$  is an  $(L+1) \times (N+1)$  matrix with the following components

$$(3.17) \quad e_{l,j}^* = \sigma(l-\frac{1}{2}) \cos(\sigma(l-\frac{1}{2})\theta_{l-1}) \left( \frac{R^*}{R} \right)^{\sigma(l-\frac{1}{2})} \times \frac{1}{2} (\Delta \theta_{l-1} + \Delta \theta_l), \quad (3.17)$$

$1 \leq l \leq L+1$  and  $1 \leq j \leq N+1$ .

We now have

$$(3.18) \quad ED^{-1}E^T = \begin{pmatrix} 0 & 0 \\ 0 & T \end{pmatrix}, \quad (3.18)$$

with  $T = E^* D^{-1} (E^*)^T$ , and

$$(3.19) \quad \lambda \max(ED^{-1}E^T) = \lambda \max(T) = \lambda \max(E^* D^{-1} (E^*)^T). \quad (3.19)$$

Moreover, the components  $T_{i,j}$  of  $T$  can be obtained from (3.6), (3.17) and (3.18).

$$(3.20) \quad \begin{aligned} T_{i,j} &= \sum_{l=1}^{L+1} \frac{e_{l,i}^* e_{l,j}^*}{d_{l,i}} = \frac{1}{2\Theta} \sum_{l=0}^{L+1} \sigma(l-\frac{1}{2}) \cos(\sigma(l-\frac{1}{2})\theta_{l-1}) \cos(\sigma(l-\frac{1}{2})\theta_{j-1}) \\ &\quad \times (\Delta \theta_{l-1} + \Delta \theta_{l-2}) (\Delta \theta_{j-1} + \Delta \theta_{j-2}). \end{aligned} \quad (3.20)$$

Hence, we have from (2.41)

$$(3.21) \quad |T_{i,j}| \leq Ch^2 L^2, \quad 1 \leq i, j \leq N+1. \quad (3.21)$$

The maximal eigenvalue of the  $(N+1) \times (N+1)$  matrix  $T$  can be bounded by

$$\lambda_{\max}(T) \leq \max_j \sum_{i=1}^{N+1} |T_{ij}| \leq ChL^2 \quad (3.21)$$

The desired result (3.14) follows from (3.19) and (3.21).  $\square$

The following corollary is directly reduced from Theorem 7.

**Corollary 8.** *Let all conditions in Theorem 7 hold. Also suppose that the coupling relations (2.40), (2.42) or (2.43) are used, then there exist bounds*

$$\text{con. num.}(D) = O(h^{-2}), \quad \text{con. num.}(F) = O(h^{-2}). \quad (3.22)$$

We note that the asymptotic relations in (3.22) are exactly the same as in the finite-element method [22], and also are better results than those in the nonconforming methods [13]. Now we can see how significant the coupling strategy of (2.40), (2.42) or (2.43) is! With this coupling strategy, not only the optimal convergence rates (2.38) can be obtained, but also the optimal asymptotic rates (3.22) of condition numbers can be achieved.

#### 4. Numerical experiments for Motz's problem

In this section, the simplified hybrid-combined method is applied to the singular Motz problem [12, 19, 23, 24, 26] that seeks a solution to satisfy the Laplace equation (see Fig. 3)

$\Delta u = 0$  in  $S$ , where  $S$  is the domain in Fig. 4. The boundary conditions are  $u = 0$  on  $\partial S_1$  and  $\partial S_2$ , and  $\partial u / \partial n = 0$  on  $\partial S_3$ . The domain  $S$  is a quarter-circle with radius 1, centered at the origin, and the boundary  $\partial S_1$  is the part of the circle in the first quadrant,  $\partial S_2$  is the part of the circle in the second quadrant, and  $\partial S_3$  is the part of the circle in the third quadrant.

The domain  $S$  is divided into two subdomains  $S_1$  and  $S_2$  by the line  $x = 0$ . The boundary  $\partial S_1$  is the part of the circle in the first quadrant,  $\partial S_2$  is the part of the circle in the second quadrant, and  $\partial S_3$  is the part of the circle in the third quadrant. The boundary  $\partial S_1$  is the part of the circle in the first quadrant,  $\partial S_2$  is the part of the circle in the second quadrant, and  $\partial S_3$  is the part of the circle in the third quadrant.

The boundary  $\partial S_1$  is the part of the circle in the first quadrant,  $\partial S_2$  is the part of the circle in the second quadrant, and  $\partial S_3$  is the part of the circle in the third quadrant.

The boundary  $\partial S_1$  is the part of the circle in the first quadrant,  $\partial S_2$  is the part of the circle in the second quadrant, and  $\partial S_3$  is the part of the circle in the third quadrant.

The boundary  $\partial S_1$  is the part of the circle in the first quadrant,  $\partial S_2$  is the part of the circle in the second quadrant, and  $\partial S_3$  is the part of the circle in the third quadrant.

The boundary  $\partial S_1$  is the part of the circle in the first quadrant,  $\partial S_2$  is the part of the circle in the second quadrant, and  $\partial S_3$  is the part of the circle in the third quadrant.

The boundary  $\partial S_1$  is the part of the circle in the first quadrant,  $\partial S_2$  is the part of the circle in the second quadrant, and  $\partial S_3$  is the part of the circle in the third quadrant.

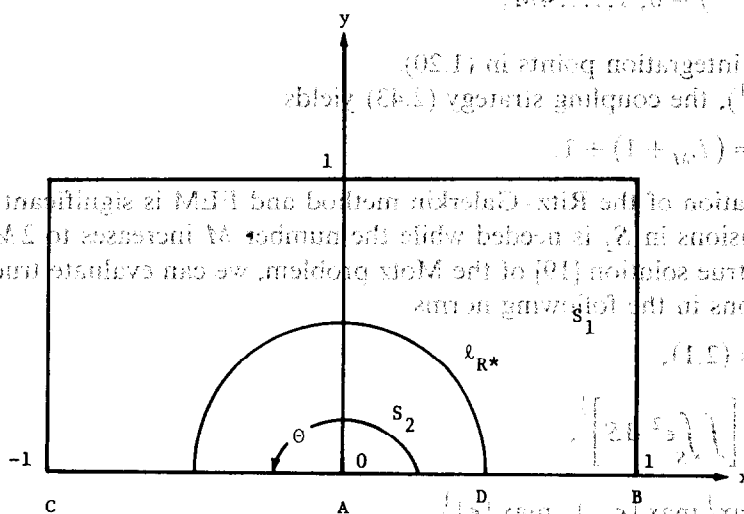


Fig. 3. Motz's problem.

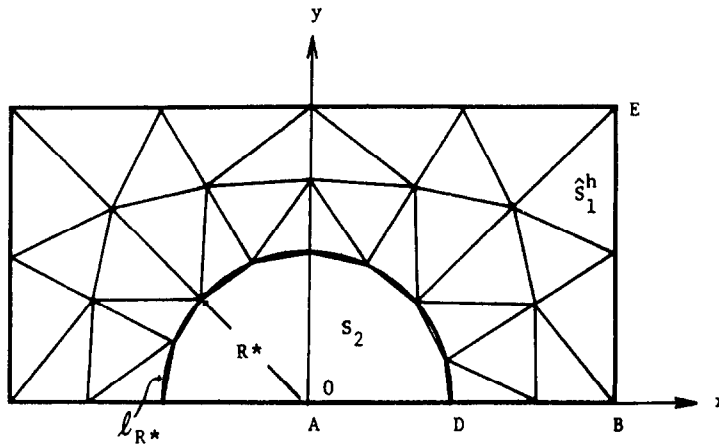


Fig. 4. The division for Motz's problem with  $M = 2$  and  $R^* = 0.5$ .

and the mixed type of Dirichlet–Neumann boundary conditions

$$u|_{x < 0 \cap y = 0} = 0, \quad u|_{x=1} = 500, \quad (4.1b)$$

$$\frac{\partial u}{\partial y} \Big|_{y=1} = \frac{\partial u}{\partial y} \Big|_{y=0 \cap x > 0} = \frac{\partial u}{\partial x} \Big|_{x=-1} = 0, \quad (4.1c)$$

where  $S$  is a rectangle  $(-1 < x < 1, 0 < y < 1)$ .

We note that there exists a singular point  $(0, 0)$ , the intersection point of the Dirichlet–Neumann boundary conditions. In this case,  $\Theta = \pi$ , i.e.,  $\sigma = \pi/\Theta = 1$ . A division of combination is given in Fig. 4 where  $R = 1$  and  $R^* = \frac{1}{2}$ . Then  $R^*/R = \frac{1}{2}$ . Denote  $M$  as the element numbers along both boundaries  $\overline{DB}$  and  $\overline{BE}$  in Fig. 4, in an equidistribution. We let the element nodes  $(R^*, \theta_j)$  on  $l_{R^*}$  also be in an equidistribution with

$$\theta_j = \frac{j\pi}{4M}, \quad j = 0, 1, \dots, 4M, \quad (4.2)$$

and let  $(R^*, \theta_j)$  be integration points in (1.20).

Since  $h = O(M^{-1})$ , the coupling strategy (2.43) yields

$$L_{2M} + 1 = (L_M + 1) + 1. \quad (4.3)$$

This coupling relation of the Ritz–Galerkin method and FEM is significant because only one more term of expansions in  $S_2$  is needed while the number  $M$  increases to  $2M$ !

By means of the true solution [19] of the Motz problem, we can evaluate true errors  $\epsilon = u - \hat{u}_h$  of numerical solutions in the following norms

$$\|\epsilon\|_h \quad \text{as (2.1)}, \quad (4.4a)$$

$$\|\epsilon\|_{0,S} = \left[ \int \int_S \epsilon^2 dS \right]^{\frac{1}{2}}, \quad (4.4b)$$

$$\text{Max} = \max \left\{ \max_{\hat{S}_1^h} |\epsilon_{i,j}|, \max_{S_2} |\epsilon| \right\}, \quad (4.4c)$$



Table 1

The error norms of numerical solutions for  $M = 2$  and  $R^* = 0.5$  while changing  $L + 1$ 

$L + 1$	$\ \epsilon^+ - \epsilon^-\ _{\infty, l_{R^*}}$	$\ \epsilon^+ - \epsilon^-\ _{0, l_{R^*}}$	Max	$\ \epsilon\ _{0, S}$	$\ \epsilon\ _h$
2	7.370	5.255	5.075	2.851	36.41
3	2.471	1.644	3.345	2.419	35.56
4	1.169	0.7191	4.221	2.414	35.53
5	1.246	0.7275	4.217	2.416	35.53
6	1.196	0.7284	4.212	2.417	35.53
8	1.257	0.7284	4.211	2.417	35.53
10	1.218	0.7274	4.211	2.417	35.53
14	1.477	0.8907	4.228	2.417	35.52
16	13.60	9.114	4.259	4.534	37.39

$$\|\epsilon^+ - \epsilon^-\|_{0, l_{R^*}} = \left[ \int_{l_{R^*}} (\epsilon^+ - \epsilon^-)^2 dl \right]^{\frac{1}{2}}, \quad (4.4d)$$

$$\|\epsilon^+ - \epsilon^-\|_{\infty, l_{R^*}} = \max_{l_{R^*}} |\epsilon^+ - \epsilon^-|. \quad (4.4e)$$

First, we take the division of Fig. 4 where  $M = 2$  as a model to be calculated in changing the total number  $L + 1$ . The simplified hybrid-combined method (1.21) with integration approximation (1.20) is used. Error norms and approximate coefficients  $\hat{D}_l$  are provided in Tables 1 and 2. It can be viewed that the total number  $L + 1 = 4$  is an optimal choice for  $M = 2$  because of small error norms and the least calculation work.

Next, we refine the division of Fig. 4 by increasing the number  $M$  of elements. Based on the coupling relation (4.3) and a pair of optimal matches known,  $L + 1 = 4$  and  $M = 2$ , we can deduce other pairs of optimal matches

$$L + 1 = 5 \quad \text{for } M = 4, \quad L + 1 = 6 \quad \text{for } M = 8. \quad (4.5)$$

The results are also given in Tables 3 and 4, by which we draw curves of error norms in Figs.

Table 2

The calculated coefficients for  $M = 2$  and  $R^* = 0.5$  while changing  $L + 1$ 

$L + 1$	$\hat{D}_0$	$\hat{D}_1$	$\hat{D}_2$	$\hat{D}_3$	$\hat{D}_5$	$\hat{D}_7$	$\hat{D}_{11}$	$\hat{D}_{15}$
2	398.951	88.0557						
3	399.174	88.2432	18.7774					
4	399.172	88.2237	18.7449	-11.8927				
5	399.173	88.2229	18.7438	-11.8952				
6	399.173	88.2193	18.7458	-11.8940	3.44176			
8	399.174	88.2203	18.7416	-11.8971	3.41371	3.38041		
10	399.174	88.2201	18.7422	-11.8965	3.41766	1.45073		
14	399.170	88.2182	15.5612	-8.97259	2.02097	1.42134	-17.1838	
16	386.391	79.5218	15.5445	-8.97711	2.04137	1.40775	-17.1640	13175.1
True coefficients								
[19]	401.162	87.6559	17.2379	-8.07122	0.331055	-0.086933	-0.00031841	-0.00012005

Table 3

The error norms of numerical solutions for  $R^* = 0.5$ ,  $L = 4$  and  $S = M$  with hybrid technique for approximating the error norms

Divisions	$\ \epsilon^+ - \epsilon^-\ _{\infty, \Gamma_R^*}$	$\ \epsilon^+ - \epsilon^-\ _{0, \Gamma_R^*}$	Max	$\ \epsilon\ _{0, S}$	$\ \epsilon\ _h$
$M = 2, L + 1 = 4$	1.16982	0.7191	4.221	2.414	35.53
$M = 3, L + 1 = 5$	0.5617	0.3563	1.941	1.032	23.30
$M = 4, L + 1 = 6$	0.3615	0.2197	1.102	0.5729	17.39
$M = 6, L + 1 = 8$	0.1848	0.1116	0.4876	0.2526	11.56
$M = 8, L + 1 = 10$	0.1114	0.06822	0.2744	0.1417	8.663

5–7. It can be seen that there appear the following asymptotic relations:

$$\|\epsilon\|_h = O(h), \quad (4.6a)$$

$$\|\epsilon\|_{0, S} = O(h^2), \quad (4.6b)$$

$$\max = O(h^2), \quad (4.6c)$$

$$\|\epsilon^+ - \epsilon^-\|_{0, \Gamma_R^*} = O(h^3), \quad (4.6d)$$

$$\|\epsilon^+ - \epsilon^-\|_{\infty, \Gamma_R^*} = O(h^3), \quad (4.6e)$$

$$\delta D_i = |\hat{D}_i - \bar{D}_i| = O(h^2), \quad i = 0, 1, 2. \quad (4.6f)$$

Evidently, (4.6a–c) are consistent with those in FEM [1,4,22]. In particular, the numerical result (4.6a) agrees with the above theoretical analyses.

Let us compare (4.6) with those in [13]. The error norms (4.6d,e) on the common boundary  $\Gamma_0$  have a little lower order  $O(h^3)$  of convergence rates than  $O(h^2)$  in [13]. This can be explained by the fact that the simplified hybrid techniques (1.18) are not very strong constraints between  $v^+$  and  $v^-$  as the direct conditions  $v_8^+ = v_8^-$  on  $(R^*, \theta_j)$  in [13]. However, the approximate coefficients  $\hat{D}_0, \hat{D}_1, \hat{D}_2$  obtained still have a good convergence rate (4.6f). When  $M = 8$  and  $L + 1 = 10$ , the value of  $\hat{D}_0$  is

$$\hat{D}_0 = 401.037 \quad (4.7)$$

with a small relative error 0.0003. It is spectacular that the value of  $\hat{D}_0$  in (4.7) is exactly the same as that in the nonconforming combinations [13].

Table 4

The calculated coefficients for  $R^* = 0.5$ 

Divisions	$\hat{D}_0$	$\hat{D}_1$	$\hat{D}_2$	$\hat{D}_3$	$\hat{D}_4$	$\hat{D}_5$
$M = 2, L + 1 = 4$	399.172	88.2237	18.7449	11.8927	6.0588	3.1696
$M = 3, L + 1 = 5$	400.285	87.8612	17.9537	10.3167	5.1366	2.6581
$M = 4, L + 1 = 6$	400.666	87.7659	17.6624	9.5290	4.5175	2.298
$M = 6, L + 1 = 8$	400.940	87.7044	17.4375	8.81086	4.0175	2.069337
$M = 8, L + 1 = 10$	401.037	87.6834	17.3532	8.51183	3.66907	1.857042
True coefficients [19]	401.162	87.6559	17.2379	8.07122	3.44027	3.31055

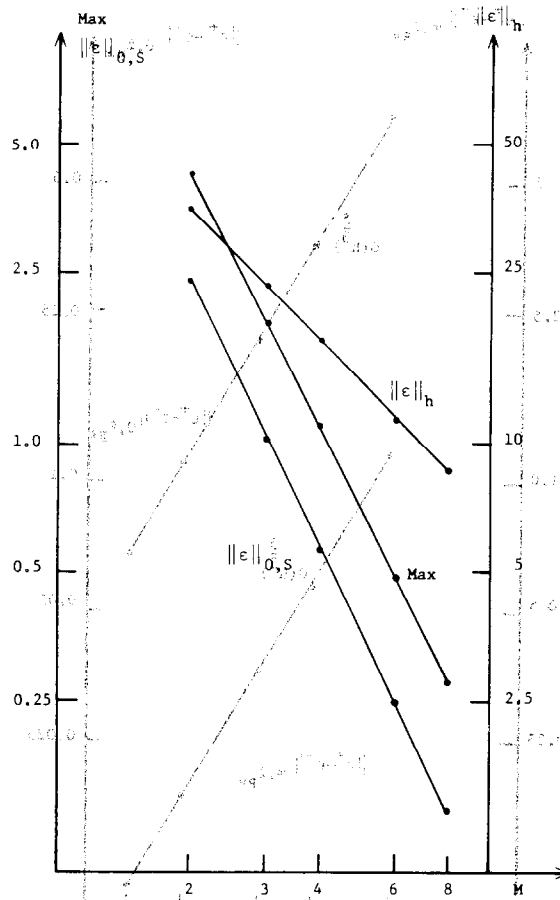


Fig. 5. Curves of error norms  $\|\epsilon\|_h$ ,  $\|\epsilon\|_{0,S}$  and Max versus  $M$ .

### Concluding remarks

(1) The homogeneous equation in  $S_2$ , e.g., the Laplace equation

$$\Delta u = 0 \quad \text{in } S_2,$$

is a necessary condition for the optimal rate of convergence owing to (2.11) (see [18]).  $S_2$  is the subdomain using the Ritz–Galerkin method with particular solutions. For the nonhomogeneous equations, e.g., the Poisson equation

$$\Delta u = f \quad \text{in } S_2,$$

suppose that we can find a particular solution  $u^*$  such that (see the expansion approaches in [22])

$$\Delta u^* = f \quad \text{in } S_2.$$

Consequently, let  $w = u - u^*$ , we also obtain the homogeneous equation

$$\Delta w = 0 \quad \text{in } S_2,$$

which can be solved by the method in this paper.

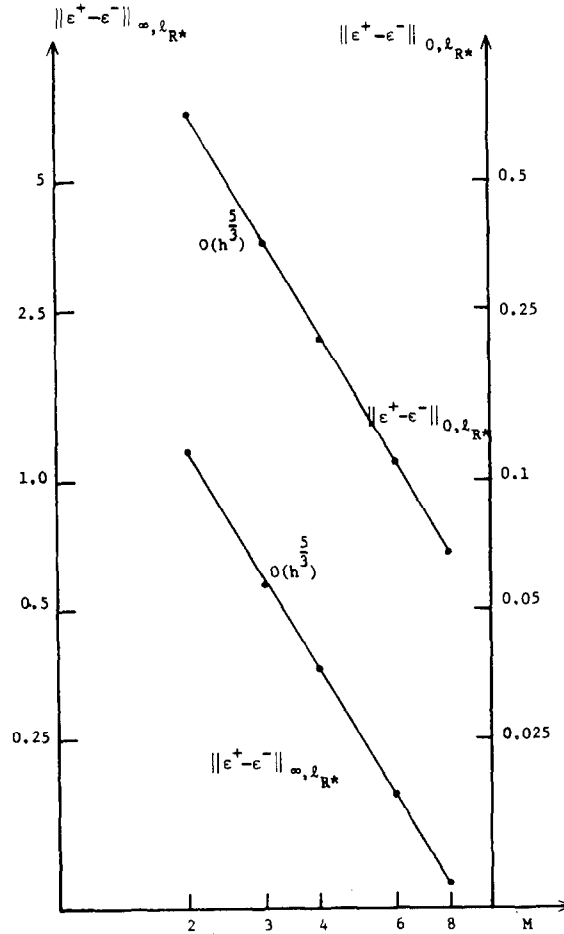


Fig. 6. Curves of  $\|\epsilon^+ - \epsilon^-\|_{0, L_{R*}}$  and  $\|\epsilon^+ - \epsilon^-\|_{\infty, L_{R*}}$  versus  $M$ .

(2) The homogeneous conditions (1.2) and (1.3), and the conditions

$$u|_{x < 0 \cap y = 0} = \frac{\partial u}{\partial y} \Big|_{y = 0 \cap x > 0} = 0 \quad (4.12)$$

in (4.1) are important for the analyses in this paper. Assume the nonhomogeneous boundary conditions given by

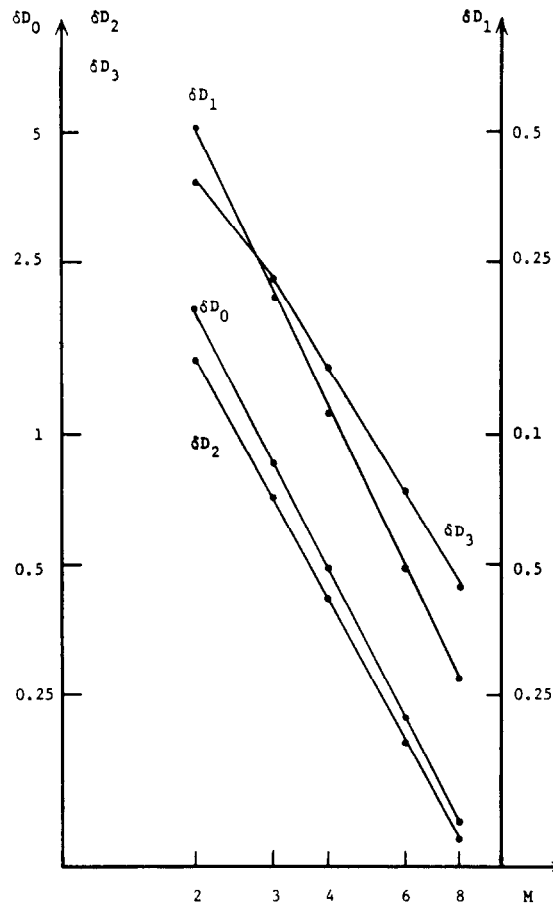
$$u|_{x < 0 \cap y = 0} = f_1(r), \quad \frac{\partial u}{\partial y} \Big|_{y = 0 \cap x > 0} = g_1(r) \quad (4.13)$$

for the Motz problem. We can use a transformation

$$u = w + f_1(r) + g_1(r)(\theta - \pi) \quad (4.14)$$

to obtain the homogeneous conditions

$$w|_{x < 0 \cap y = 0} = \frac{\partial w}{\partial y} \Big|_{y = 0 \cap x > 0} = 0 \quad (4.15)$$

Fig. 7. Curves of errors  $\delta D_i$  versus  $M$ .

and the Poisson equation

$$\Delta w = f, \quad (4.16a)$$

where

$$f = \Delta(f_1(r) + g_1(r)(\theta - \pi)). \quad (4.16b)$$

By noting remark (1), equations (4.16) may be substituted by using the Laplace equation in  $S_2$  with the help of another transformation.

(3) In [16] we have discussed a general, hybrid-combined technique with the following additional integral on  $\Gamma_0$

$$\int_{\Gamma_0} \left( \alpha \frac{\partial u^+}{\partial n} + \beta \frac{\partial u^-}{\partial n} \right) (v^+ - v^-) \, dl - \int_{\Gamma_0} \left( \alpha \frac{\partial v^-}{\partial n} + \beta \frac{\partial v^+}{\partial n} \right) (u^+ - u^-) \, dl \quad (4.17)$$

instead of (1.18), where  $\alpha$  and  $\beta$  are real,  $\alpha + \beta = 1$ . It can be seen in [16] that the simplified hybrid technique with (1.18) is a special case of (4.17) while  $\alpha = 1$  and  $\beta = 0$ . Numerical

experiments prove that the current coupling technique as (1.18) is best among those using (4.17), for the error norms and condition numbers of the numerical solutions obtained. This implies the significance of the theoretical analyses in this paper.

## Acknowledgements

We would like to thank the referees for their valuable comments and careful reading of the manuscript.

## References

- [1] I. Babuška and A.K. Aziz, Survey lectures on the mathematical foundations of the finite element method, in: A.K. Aziz, Ed., *Mathematical Foundations of the Finite Element Method with Applications to Partial Differential Equations* (Academic Press, New York, 1972) 3–359.
- [2] I. Babuška and B.Q. Guo, The *hp*-version of the finite element method for domains with curved boundaries, *SIAM J. Numer. Anal.* **25** (1988) 837–861.
- [3] H. Blum and H. Dobrowolski, On finite element method for elliptic equations on domains with corners, *Computing* **28** (1982) 53–63.
- [4] P.G. Ciarlet, *The Finite Element Methods for Elliptic Problems* (North-Holland, Amsterdam, 1978).
- [5] L.M. Delves and C.A. Hall, An implicit matching principle for global element calculation, *J. Int. Math. Appl.* **23** (1979) 223–234.
- [6] G. Fix, S. Gulati and G.I. Wakoff, On the use of singular functions with finite element approximations, *J. Comp. Phys.* **13** (1973) 209–238.
- [7] C.I. Goldstein, The finite element method with nonuniform mesh size applied to the exterior Helmholtz problem, *Numer. Math.* **38** (1981) 61–82.
- [8] C.I. Goldstein, A finite element method for solving Helmholtz type equations in waveguides and other unbounded domains, *Math. Comp.* **38** (1982) 309–324.
- [9] H. Han, The numerical solution of interface problem in infinite element method, *Numer. Math.* **39** (1982) 39–50.
- [10] C. Johnson and C. Nédélec, On the coupling of boundary integral and finite element methods, *Math. Comp.* **35** (1983) 1063–1079.
- [11] R.S. Lehman, Developments of analytic solutions of elliptic partial differential equations, *J. Math. Mech.* **8** (1959) 727–760.
- [12] Z.C. Li, An approach for combining the Ritz–Galerkin and finite element methods, *J. Approx. Theory* **39** (1983) 132–152.
- [13] Z.C. Li, A nonconforming combined method for solving Laplace's boundary value problems with singularity problems, *Numer. Math.* **49** (1986) 475–497.
- [14] Z.C. Li, Numerical methods for elliptic boundary value problems with singularities, Ph.D. thesis, Dept. Math. Appl. Math., Univ. Toronto, May 1986.
- [15] Z.C. Li and T.D. Bui, A new kind of combination between the Ritz–Galerkin and finite element methods for singularity problems, *Computing* **40** (1988) 29–50.
- [16] Z.C. Li and T.D. Bui, Generalized hybrid-combined methods for the singularity problems of homogeneous elliptic equations, *Internat. J. Numer. Methods Engrg.* **26** (1988) 788–803.
- [17] Z.C. Li and T.D. Bui, Six combinations of the Ritz–Galerkin and finite element methods for elliptic boundary value problems, *Numer. Methods for P.D.E.* **4** (1988) 197–218.
- [18] Z.C. Li and G.P. Liang, On the simplified hybrid-combined method, *Math. Comp.* **41** (1983) 13–25.
- [19] Z.C. Li, R. Mathon and P. Sierrier, Boundary methods for solving elliptic problems with singularities and interfaces, *SIAM J. Numer. Anal.* **24** (1987) 487–498.

- [20] J.L. Lions and E. Magénes, *Problèmes aux Limites non Homogènes et Applications, Vol. I.*, Travaux et Recherches Mathématique **17** (Dunod, Paris, 1968).
- [21] S.L. Sobolev, *Application of Functional Analysis in Mathematical Physics*, Trans. Math. Monographs 7 (Amer. Mathematical Soc., Providence, R.I., 1963).
- [22] G. Strang and G.J. Fix, *An Analysis of the Finite Element Method* (Prentice-Hall, Englewood Cliffs, NJ, 1973).
- [23] R.W. Thatcher, The use of infinite grid refinement at singularities in the solution of Laplace's equation, *Numer. Math.* **25** (1976) 163–178.
- [24] J.R. Whiteman and N. Papanichael, Treatment of harmonic mixed boundary value problems by conformal transformation methods, *Z. Angew. Math. Phys.* **23** (1972) 655–664.
- [25] N.M. Wigley, Asymptotic expansions at a corner of solutions of mixed boundary value problems, *J. Math. Mech.* **4** (1964) 569–576.
- [26] N.M. Wigley, An efficient method for subtracting off singularities at corners for Laplace's equation, *J. Comp. Phys.* **78** (1988) 368–376.
- [27] A.P. Zielinski and O.C. Zienkiewicz, Generalized finite element analysis with T-complete boundary solution function, *Internat. J. Numer. Methods Engrg.* **21** (1985) 509–528.
- [28] C. Zienkiewicz, D.W. Kelly and P. Betters, The coupling of the finite element method and boundary solution procedures, *Internat. J. Numer. Methods Engrg.* **11** (1977) 335–375.